Available online at www.sciencedirect.com

SCIENCE DIRECT®

Catalysis Today 89 (2004) 313–318

CATALYSIS TODAY

www.elsevier.com/locate/cattod

Inelastic neutron scattering and migration energies in FePd

T. Mehaddene[a], M. Zemirli[a], V. Pierron-Bohnes[b,*], M.C. Cadeville[b],
B. Hennion[c], A. Marty[d], I. Schuster[d], K. Tanaka[e], H. Numakura[e]

[a] *LPCQ, Université Mouloud Mammeri, 15000 Tizi-Ouzou, Algeria*
[b] *IPCMS, 23 rue du Loess, F-67037 Strasbourg, France*
[c] *LLB, CEA Saclay, F-91191 Gif sur Yvette Cedex, France*
[d] *CENG, 17 avenue des martyrs, F-38054 Grenoble Cedex 09, France*
[e] *Department of Materials Science and Engineering, Sakyo-ku, Kyoto 6068501, Japan*

Abstract

The frequencies of the normal modes of vibration of FePd single crystal have been measured using inelastic neutron scattering. The measurements were performed for the $L1_0$ ordered structure at 300 and 860 K and for the fcc disordered state at 1020 K. A general lowering of phonon frequencies with increasing temperature is found in FePd, the dependence being the strongest for acoustical transverse $[\xi\,\xi\,\xi]$ branches. The migration energies as well as several thermodynamic quantities have been calculated from the densities of states. The contribution of ordering to the migration energy, as experimentally determined in this work, agrees well with the obtained one by Monte Carlo simulations in the $L1_0$ structure.

Keywords: Vibration of FePd; Inelastic neutron scattering; $L1_0$ structure

---

1. Introduction

Intermetallics form an important class of materials, and among them those presenting a phase diagram derived from the AuCu canonical phase diagram are of outstanding technological importance. After a period of strong research on superalloys for their magnetic [1–5], catalytic [6] and high temperature mechanical [7] properties, nowadays some of them arouse a new interest owing to their possible applications as shape memory alloys [8] and high density recording media because of their large magnetic anisotropy [9,10]. A good knowledge of the ordering processes and of its dynamics is thus a necessary step in any extensive research on those systems.

The FePd system has recently given rise to many studies as magnetic media [11,12] and shape memory candidate [8]. The FePd system exhibits a phase transition between the disordered fcc phase and the $L1_0$ (CuAu(I) type) ordered tetragonal structure around 920 K at the equiatomic composition. The ordered structure is based on the fcc lattice and consists of alternating planes of Fe and Pd atoms. This very anisotropic chemical ordering is accompanied by a tetragonalization of the lattice ($c/a < 1$) and a magnetic anisotropy.

Among the two energetic parameters that drive self-diffusion and ordering kinetics in ordered intermetallic compounds, i.e. E_F, the vacancy formation energy, and E_M, the vacancy migration energy, E_M is generally less known and more difficult to measure. A model relating the migration energy for nearest-neighbor jumps in cubic metals to the phonon density of state has been proposed by Schober et al. [13]. In pure fcc metals, excellent agreement between calculated and measured values of E_M was found, whereas in bcc metals, where the experimental values are less well known, predictions were obtained that show a pronounced chemical group systematics. More recently the same method has been used by Randl et al. [14] in $Fe_{1-x}Si_x$ and Kentzinger et al. [15] in $Fe_{1-x}Al_x$ alloys to estimate the migration energies. Strictly speaking, this method to determine E_M is valid only for monoelemental structures. In this paper, we will use the Schober's model in order to estimate the effects of temperature and order state on the migration energy in the FePd system. The prerequisite for such an evaluation of E_M is the knowledge of the phonon dispersion for the different states of order.

---

[*] Corresponding author. Tel.: +33-88-10-7066; fax: +33-88-10-7249.
E-mail addresses: veronique.pierron-bohnes@0ipcms.u-strasbg.fr, vero@0ipcms.u-strasbg.fr (V. Pierron-Bohnes).

0920-5861/$ – see front matter © 2003 Elsevier B.V. All rights reserved.
doi:10.1016/j.cattod.2003.12.007

This paper is organized as follows. In Section 2, we report some experimental details and the results of phonon measurement. Section 3 describes the Born-von Karman model in terms of analysis of the force constants, total and weighted densities of states. The models used to calculate the migration energy, with their results are presented in Section 4. Conclusions are drawn in Section 6.

2. Phonon measurements

Inelastic neutron scattering measurements were performed on the 2T1 3-axes spectrometer near Orphée reactor of the Laboratoire Léon Brillouin (LLB) using a parallelepiped single crystal with faces parallel to the $\{1\,0\,0\}$ crystallographic planes. Further experimental details are reported in a forthcoming publication [16].

Phonon frequencies have been measured along the high symmetry directions: [1 0 0], [1 1 0] and [1 1 1] directions in both ordered and disordered phases. In the $L1_0$ phase, [0 0 1] and [1 0 1] directions, not equivalent to the [1 0 0] and [1 1 0] directions, have also been measured. The phonon dispersion curves are reported in Figs. 1–4 (in all cases, the notations of the fcc phase have been used).

The elementary unit cell of $L1_0$ FePd is tetragonal with two atoms per cell (one at the corners and one at the center). Thus six branches, three acoustical and three optical, can be measured at each **q** (position in the reciprocal space). The transversal branches are degenerated along the [0 0 1] direction in the $L1_0$ state (Fig. 1) and along the [0 0 1] and [1 1 1] directions in the fcc phase (Fig. 4). As a general trend, an overall decrease of the frequencies with increasing temperature is observed. The decrease is stronger in the case of the optical $[0\,0\,\xi]$ and $[\xi\,\xi\,0]$ branches: the lattice becomes softer as the temperature increases. The lower frequency modes,

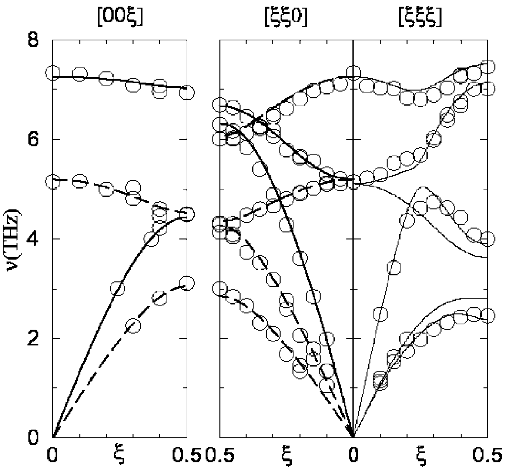

Fig. 1. Dispersion curves in the high symmetry directions at room temperature ($L1_0$ phase). The open circles correspond to the experimental data, the thick solid, dashed, and thin solid lines to the BVK fits of the longitudinal, transversal and mixed modes, respectively.

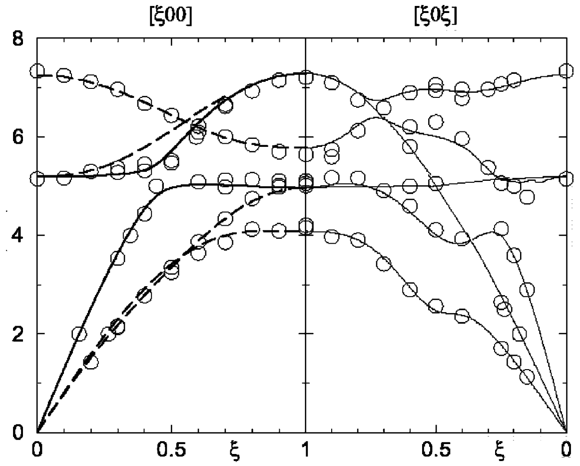

Fig. 2. Dispersion curves in the $[\xi\,0\,0]$ and $[\xi\,0\,\xi]$ directions at room temperature ($L1_0$ phase) with the same symbols as in Fig. 1.

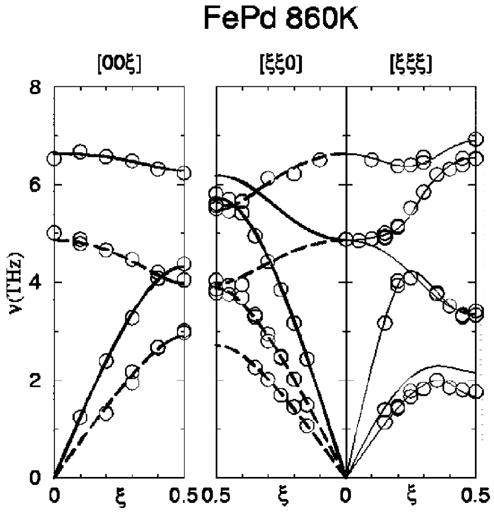

Fig. 3. Dispersion curves in the $L1_0$ phase at 860 K with the same symbols as in Fig. 1.

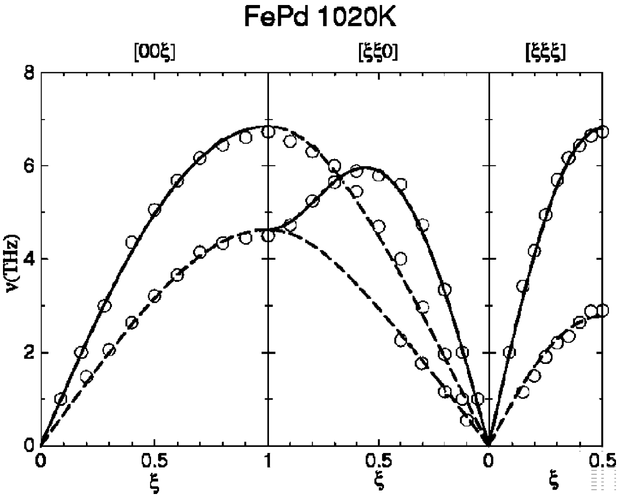

Fig. 4. Dispersion curves in the fcc phase at 1020 K with the same symbols as in Fig. 1.

the acoustical transverse branches in the [1 1 1] direction, seem to be more affected by the increasing temperature. Those branches shift a lot between 860 K and room temperature (about 1 THz at the zone boundary). As expected, the main difference between the two states of order is that new branches (optical modes around 6–7 THz) appear in the $L1_0$ phase due to the increase of atom number per elementary unit cell. However, the separation between the acoustical and optical branches is not sufficient to create a gap in the densities of states.

The general aspect of the dispersion curves in the $L1_0$ ordered phase is quite similar to that obtained by Stirling et al. [17] on Pd_3Fe measured at 80 K. A particular agreement can be observed along the [1 1 1] direction, where a maximum of the longitudinal acoustic branch is located at $\xi = 0.3$.

In the fcc disordered state, the phonon spectra display the specific features of phonon dispersion in fcc lattices: degenerated transversal branches in the [1 1 1] and [0 0 1] directions and an *extremum* of the second acoustical transverse $[\xi\,\xi\,0]$ branch localized at $\xi = 0.5$.

3. Born-von Karman fits

The measured frequencies $\nu(\mathbf{q})$ have been fitted in the harmonic approximation via the Born-von Karman model. Using the axially symmetrical force constant model first developed by Lehman et al. [18], we assume that the potential energy of the crystal is a sum of spherical two-body potentials taken over all pairs (l, l') of lattice sites. The interaction between any two atoms at any distance from each other is reduced to two force constants. Those force constants are linked to the central potential by the following relations:

$$L_n(\lambda\lambda') = -\frac{\mathrm{d}^2 V}{\mathrm{d}r_n^2} \quad \text{and} \quad T_n(\lambda\lambda') = -\frac{1}{r_n}\frac{\mathrm{d}V}{\mathrm{d}r_n} \tag{1}$$

$L_n(\lambda\lambda')$ and $T_n(\lambda\lambda')$ are, respectively, called longitudinal and transversal force constants of the *n*th nearest-neighbor interaction between atoms λ and λ'. Reasonable agreement with the experimental data was found in the $L1_0$ phase with 21 adjustable parameters (corresponding to longitudinal interactions up to the fourth nearest neighbors of the fcc structure and transversal force constants up to the second neighbors).

In the fcc phase, the number of force constants is reduced because of the higher symmetry; a set of six fitting parameters was sufficient (interactions up to third nearest neighbors of the fcc structure). In this phase, the fits were performed using the average mass of the atoms.

The results of the fits are the solid and dashed lines in Figs. 1–4. The resulting force constants are given in Tables 1 and 2. The relative error on all frequencies was estimated to be 3%. In spite of the fact that those BVK fits are mainly a useful way to interpolate the dispersion curves in the first Brillouin zone, general tendencies can be drawn. The transversal force constants are one order of magnitude smaller than the longitudinal ones. The general softening of the lattice with increasing temperature induces a general decrease of the predominant force constants. It is in this case not possible to separate the direct effects of temperature (lattice expansion, anharmonicities, etc.) from the effect due to the significant change of order.

Table 1
Longitudinal L_n and transversal T_n force constants (in N/m), from the BVK fits in the $L1_0$ phase at 300 and 860 K[a]

Neighbor	Coordinate	300 K		860 K	
		L_n	T_n	L_n	T_n
Fe–Pd$_1$	$\frac{1}{2}\,0\,\frac{1}{2}$	34.3(4)	−2.1(3)	30.6(6)	−2.5(5)
Fe–Fe$_1$	$\frac{1}{2}\,\frac{1}{2}\,0$	21.3(9)	−1.6(6)	15.4(9)	−4.1(9)
Pd–Pd$_1$	$\frac{1}{2}\,\frac{1}{2}\,0$	52.1(9)	−2.7(6)	41.8(9)	−2.9(7)
Fe–Fe$_{2z}$	0 0 1	3.4(9)	−2.4(3)	2.2(9)	−2.9(6)
Pd–Pd$_{2z}$	0 0 1	0.2(9)	−0.5(6)	2.9(7)	−1.8(2)
Fe–Fe$_{2x}$	1 0 0	1.2(6)	−2.8(5)	2.4(9)	−0.3(1)
Pd–Pd$_{2x}$	1 0 0	−0.1(9)	0.9(5)	−0.4(9)	−0.4(1)
Fe–Fe$_3$	$\frac{1}{2}\,\frac{1}{2}\,1$	0.8(5)	0.0	1.4(9)	0.0
Pd–Pd$_3$	$\frac{1}{2}\,\frac{1}{2}\,1$	1.1(6)	0.0	−0.5(3)	0.0
Fe–Pd$_3$	$\frac{1}{2}\,1\,\frac{1}{2}$	0.9(3)	0.0	0.9(4)	0.0
Fe–Fe$_{4z}$	2 0 2	4.3(5)	0.0	2.0(9)	0.0
Pd–Pd$_{4z}$	2 0 2	−0.2(6)	0.0	2.4(2)	0.0
Fe–Fe$_{4x}$	2 2 0	−2.9(6)	0.0	−0.6(9)	0.0
Pd–Pd$_{4x}$	2 2 0	3.8(9)	0.0	−2.7(9)	0.0

[a] The neighbors are indexed in the fcc structure. The notation A–B$_{nZ}$ indicates *n*th neighbor A–B pairs with *Z* orientation ($Z = x$ (equivalent to *y*) or *z*).

Using the atomic force constants obtained from the BVK fits, the total phonon density of states (DOS) $Z(\nu)$ has been obtained at each temperature from the dispersion relations $\nu_j(\mathbf{q})$ by an integration over the first Brillouin zone:

$$Z(\nu) = \frac{1}{3n}\frac{V}{(2\pi)^3}\sum_j \int \delta(\nu - \nu_j(\mathbf{q}))\,\mathrm{d}\mathbf{q} \tag{2}$$

where *V* is the volume of the unit cell and *n* the number of atoms per unit cell. The sum runs over all phonon branches *j*. The integration is carried out numerically by scanning the Brillouin zone in a way first proposed by Gilat and Raubenheimer [19]. We have also calculated the so-called weighted phonon densities of states for the atom λ: $Z_\lambda(\nu)$.

The weighted and the total densities of states at the various temperatures are shown in Fig. 5. One can see from this figure that the contribution from the heavy Pd atoms to the total frequency distribution arises mainly from the low-energy acoustical modes. As expected from the shape of the dispersion curves, for all temperature studied, no clear separation

Table 2
Force constants (in N/m), from BVK fit in the fcc phase at 1020 K

n	Coordinate	L_n	T_n
1	$\frac{1}{2}\,\frac{1}{2}\,0$	32.4(4)	−2.1(2)
2	1 0 0	−0.1(3)	−0.9(2)
3	$\frac{1}{2}\,\frac{1}{2}\,1$	0.8(1)	0.0(1)

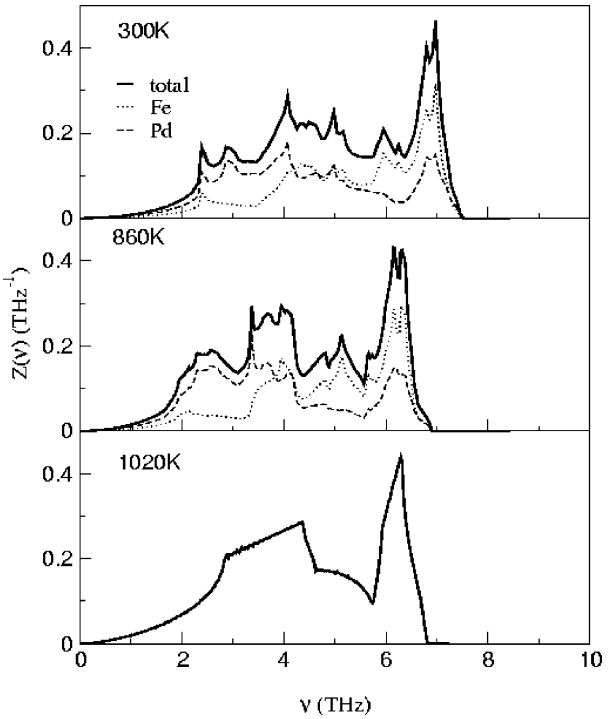

Fig. 5. Total and weighted phonon density of states of FePd at various temperatures.

between the low- and high-energy ranges is visible on the DOS graphs. At 860 K, all frequencies are shifted towards lower values. For example, the cut-off frequency diminishes from 7.5 THz at 300 K to 6.9 THz at 860 K.

4. Migration energy calculation

The migration energy has been evaluated from the phonon DOS using the model developed by Schober et al. [13]. This model was first applied successfully to pure fcc and bcc metals and recently to intermetallic compounds Fe_3Si [14] and $Fe_{1-x}Al_x$ [15] with the $D0_3$ and B2 structures. In this model, the migration energy is derived from the following relation:

$$E_M^{Sch} = 4\pi^2 a^2 \alpha G_0^{-1} \tag{3}$$

where

$$G_0 = \int \frac{Z(\nu)}{M\nu^2} d\nu$$

In (3), E_M separates into a structural factor ($a^2\alpha$) common to all fcc and to the derived $L1_2$ and $L1_0$ structures, and an electronic factor (G_0), which is the static Green function and reflects the electronic particularities of the investigated metal or alloy. a is the lattice parameter and α a geometrical constant, α has been determined by computer simulation to be equal to 0.0135 in fcc metals [13]. Strictly speaking, formula (3) is only valid for pure cubic metals. As a first approximation, we consider the FePd $L1_0$ structure as an fcc lattice with atoms of mass equal to the average mass of the two atoms.

Table 3
Elastic constants (in GPa) deduced from this phonon measurements (PM) and from ultrasonic measurements [21] (USM) in FePd at 1020 K and migration energies in the fcc disordered state, deduced from the Flynn's model (E_M^{Fly})

Technique	C_{11}	C_{12}	C_{44}	E_M^{Fly}
PM	184	130	64.5	0.78
USM	159	117	63	0.67

In the fcc disordered state, where the symmetry is cubic, one can also determine the migration energy from the elastic constants using the Flynn's [20] model on which the Schober's model was build:

$$E_M^{Fly} = C\Omega\delta^2 \tag{4}$$

where

$$\frac{15}{2C} = \frac{3}{C_{11}} + \frac{2}{C_{11} - C_{12}} + \frac{1}{C_{44}}$$

C_{11}, C_{12}, and C_{44} are the three independent elastic constants of the material, and Ω the atomic volume. δ^2 is a structure dependent constant, which has been determined such that the mean square deviation between the experimental values and E_M^{Fly} becomes minimum. Schober et al. [13] have obtained good agreement between theoretical and experimental values of the migration energy by assuming $\delta^2 = 0.081$ for the fcc structure. The elastic constants were calculated from the slopes at the origin of the phonon dispersion curves. They are also deduced from ultrasonic resonance spectrometry [21] in FePd (Table 3) performed in the disordered state at temperatures lower than 320 K and higher than 920 K. The C_{44} coefficient agrees very well with the value determined from the dispersion curves in contrast to the C_{11} and C_{12} values where there is a 10% discrepancy.

We have calculated the migration energies at the various temperatures according to Eq. (3) in the fcc phases and in the $L1_0$ structure since the Schober's model has not yet been extended to that structure. The obtained values are shown in Table 4. The migration energy decreases with increasing temperature as pure consequence of increasing anharmonicities. This between the room temperature and 860 K in the $L1_0$ phase is corroborated by recent X-rays diffraction done by one of the present authors [16]. The relative intensities of the superstructure and corresponding fundamental peaks vary significantly between 300 and 860 K, showing that the long range order is varying strongly within this temperature range.

Using a Monte Carlo model, based on a nearest-neighbor vacancy jump mechanism and on an Ising Hamiltonian with effective pair interaction energies for first- and second-neighbors in the $L1_0$ compounds, Hamidi and Kerrache [22] have found a contribution of the ordering energy to the mean migration energy equal to 0.19 meV/K close

Table 4
Migration energies deduced from the Schober's model for the average alloy and thermodynamic properties calculated in the harmonic approximation from the density of states for the different temperatures. S^{V} refers to the vibrational entropy per atom, θ_{D} to the Debye temperature, C_V to the specific heat, $\langle u_\lambda^2\rangle$ to the mean square displacement of the atom λ and B to the Debye Waller factor

T (K)	$E_{\mathrm{M}}^{\mathrm{Sch}}$ (eV)	S^{V} (k_{B}/at.)	θ_{D} (K)	C_{V} (J/mol K)	$\langle u_{\mathrm{Fe}}^2\rangle$ (Å^2)	$\langle u_{\mathrm{Pd}}^2\rangle$ (Å^2)	B (10^{-3} Å^2)
300	0.91	2.15	318.7	23.5	0.0096	0.0075	442
860	0.66	2.64	284.3	24.7	0.033	0.0291	1626
1020	0.74	2.66	286.8	24.8			1751

to $\Delta E_{\mathrm{M}}^{\mathrm{Sch}}/T_{\mathrm{c}} = 0.18$ meV/K obtained experimentally in the present work. Moreover, recently, Kozubski et al. [23] using residual resistivity measurements, have obtained a mean migration energy of 0.9 eV in the ordered phase, in good agreement with our values deduced from neutron measurements.

The migration energy at room temperature in FePd (0.91 eV) is close to the migration barriers obtained by Kentzinger and Schober [24] in $\mathrm{Pd_3Fe}$ (0.97 eV for a Pd atom migrating within its own lattice and 1.14 eV when it jumps on the Fe lattice; 0.90 eV for a Fe atom leaving its own lattice).

5. Related thermodynamic quantities

From the phonon DOS, we have calculated the vibration entropy, the Debye temperature, the mean square displacement and the specific heat within the harmonic approximation. The vibration entropy of an independent phonon gaz is given by [25]:

$$S^{\mathrm{V}} = 3k_{\mathrm{B}} \int Z(\nu)[(1+n(\nu))\ln(1+n(\nu)) - n(\nu)\ln(n(\nu))]\,\mathrm{d}\nu \quad (5)$$

where $n(\nu)$ is the Bose probability occupation and k_{B} the Boltzmann constant. The mean square displacement $\langle u_\lambda^2\rangle$ of an atom λ have been calculated according to

$$\langle u_\lambda^2\rangle = \frac{3h}{8\pi^2 M_\lambda} \int \frac{Z_\lambda(\nu)}{\nu} \coth\left(\frac{h\nu}{2k_{\mathrm{B}}T}\right) \mathrm{d}\nu \quad (6)$$

where h is the Planck's constant, M_λ the atomic mass, and T the absolute temperature. Owing to the weighting per $1/\nu$, $\langle u_\lambda^2\rangle$ is essentially determined by the low-energy phonons. The Debye Waller factor B, representing the weakening in the scattering amplitudes resulting from the thermal vibrations is deduced from the DOS according to [26]:

$$B = \frac{h}{M} \int \frac{Z(\nu)}{\nu} \coth\left(\frac{h\nu}{2k_{\mathrm{B}}T}\right) \mathrm{d}\nu \quad (7)$$

The thermodynamic quantities deduced from the above relations as well as the Debye temperature θ_{D} and the specific heat C_V are given in Table 4. The mean square displacement values reflect the atomic mass difference between Fe and Pd. The Debye temperature appears relatively sensitive to the order state: a decrease of 12% is observed on the transition from the ordered to the disordered state. As expected, the vibration entropy increases significantly (25%) with temperature. All the physical quantities related to the phonon spectra exhibit the same behavior, confirming that the effect observed on the migration energy between 300 and 860 K in FePd can be attributed to the change of the long range order.

6. Conclusions

Phonon dispersion curves in FePd single crystal have been measured in the $\mathrm{L1_0}$ ordered phase at 300 and at 860 K. The fcc disordered state was also investigated at 1020 K.

A general decrease of phonon frequencies with increasing temperature was found. An important shift with temperature was observed for the acoustical transverse branches in the [1 1 1] direction. Those modes appear at particularly low energy, indicating low potential barriers for the atomic displacements. From a Born-von Karman fit of the measured points, we have been able to calculate the phonon densities of states necessary to estimate the migration energies in FePd using the model proposed by Schober et al. [13]. The phonon DOS have also been used to calculate several thermodynamic quantities as the vibrational entropy S^{V}, the Debye temperature θ_{D}, the specific heat C_V and the Debye Waller factor B (Table 4). The contribution of ordering to the mean migration energies in FePd (0.18 meV/K) got experimentally in the present work compare well with those obtained using a Monte Carlo approach in $\mathrm{L1_0}$ compounds. As a general trend, the migration energy decreases with increasing temperature as a consequence of increasing anharmonicities.

A small increase in the migration energy is found between the partially ordered $\mathrm{L1_0}$ phase at 860 K and the fcc disordered state, but the non-cubic symmetry of the $\mathrm{L1_0}$ structure make quite rough the use of the Schober's model, valid only for the fcc and bcc pure metals. A model extended to the $\mathrm{L1_0}$ ordered structure is necessary to conclude further, it will be developed in a next future.

Acknowledgements

This work is supported partly by Algerian project ANDRU/PNR3 (AU49902) and by a collaborative program 99 MDU 449 between University Louis Pasteur of

Strasbourg, France and the University Mouloud Mammeri of Tizi-Ouzou, Algeria.

References

[1] F. Menzinger, A. Paoletti, Phys. Rev. 143 (1966) 365.
[2] G.E. Bacon, E.W. Mason, Proc. Roy. Soc. 88 (1966) 929.
[3] G.E. Bacon, J. Crangle, Proc. Roy. Soc. 272 (1963) 387.
[4] M.C. Cadeville, J.L. Moran-Lopez, Phys. Rep. 153 (1987) 331.
[5] T.H. Kim, M.C. Cadeville, A. Dinia, H. Rakoto, Phys. Rev. B 53 (1996) 221;
T.H. Kim, M.C. Cadeville, A. Dinia, V. Pierron-Bohnes, H. Rakoto, Phys. Rev. B 54 (1996) 3408.
[6] S. Zyade, F. Garin, G. Maire, New J. Chem. 11 (1987) 429.
[7] M. Morinaga, J. Saito, N. Yukawa, H. Adachi, Acta Met. Mater. 38 (1990) 25.
[8] K. Tanaka, T. Ichitsudo, M. Koiwa, Mater. Sci. Eng. A 312 (2001) 118;
K. Morioka, K. Tanaka, in: S. Hanada, Z. Zhong, S.W. Nam, R.N. Wright (Eds.), Proceedings of the Fourth Pacific Rim International Conference on Advanced Materials and Processing (PRICM4), The Japan Institute of Metals, 2001.
[9] G.R. Harp, D. Weller, T.A. Rabedeau, R.F.C. Farrow, M.F. Toney, Phys. Rev. Lett. 71 (1993) 2493.
[10] D. Weller, H. Brändle, C. Chappert, J. Magn. Magn. Mater. 121 (1993) 461.
[11] V. Gehanno, A. Marty, B. Gilles, Y. Samson, Phys. Rev. B 55 (1997) 12552.
[12] P. Kamp, A. Marty, B. Gilles, R. Hoffmann, M. Marchesini, M. Belakhovsky, C. Boeglin, H.A. Dürr, S.S. Dhesi, G. van der Laan, A. Rogalev, Phys. Rev. B 59 (1999) 1105.
[13] H.R. Schober, W. Petry, J. Trampeneau, J. Phys.: Condens. Matter 4 (1992) 9321.
[14] O.G. Randl, G. Vogl, W. Petry, B. Hennion, B. Sepiol, K. Nembach, J. Phys.: Condens. Matter 7 (1995) 5983;
O.G. Randl, PhD Dissertation, University of Vienna, 1994.
[15] E. Kentzinger, M.C. Cadeville, V. Pierron-Bohnes, W. Petry, B. Hennion, J. Phys.: Condens. Matter 8 (1996) 5535.
[16] T. Mehaddene, E. Kentzinger, B. Hennion, K. Tanaka, H. Numakura, A. Marty, V. Parasote, M.C. Cadeville, M. Zemirli, V. Pierron-Bohnes, Phys. Rev. B, submitted for publication.
[17] W.G. Stirling, R.A. Cowley, M.W. Stringfellow, J. Phys. F: Met. Phys. 2 (1972) 421.
[18] G.W. Lehman, T. Wolfram, R.E. De Wames, Phys. Rev. B 15 (1962) 1593.
[19] G. Gilat, L.J. Raubenheimer, Phys. Rev. 144 (1966) 390.
[20] C.P. Flynn, Phys. Rev. 177 (1968) 682.
[21] T. Ichitsubo, PhD Thesis, Kyoto University, 2000.
[22] M. Hamidi, A. Kerrache, Personal communication.
[23] R. Kozubski, Private communication.
[24] E. Kentzinger, H.R. Schober, J. Phys.: Condens. Matter 12 (2000) 8145.
[25] B. Diu, C. Guthman, D. Lederer, B. Roulet, Statistical Physics, Hermann, Paris, 1989.
[26] M.A. Krivoglaz, Theory of X-ray and Thermal Neutron Scattering by Real Crystals, Plenum Press, New York, 1969, Chapter 6, p. 220.